European Food Research and Technology (2021) 247:2227–2237
https://doi.org/10.1007/s00217-021-03783-1

ORIGINAL PAPER

A novel Angiotensin-I-converting enzyme (ACE) inhibitory peptide IAF (Ile-Ala-Phe) from pumpkin seed proteins: in silico screening, inhibitory activity, and molecular mechanisms

Fuqiang Liang[1] · Yumeng Shi[1] · Jiayi Shi[1] · Tai Zhang[1] · Ran Zhang[1]

Received: 7 April 2021 / Revised: 18 May 2021 / Accepted: 22 May 2021 / Published online: 3 June 2021

Abstract

Pumpkin seed proteins with desirable nutritional properties have attracted great interest as an innovative source of bioactive peptides with beneficial effects in recent years. The current study aimed to screen novel ACE inhibitory peptides from pumpkin seed proteins by in silico approach and further elucidate the underlying inhibition mechanisms. A novel tripeptide, IAF (Ile-Ala-Phe) with acceptable bioavailability properties exhibited considerable ACE inhibitory ability with an IC_{50} of 19.87 ± 0.50 μM. Molecular docking study showed that IAF could bound with key residues in the active site of ACE. Further molecular dynamics (MD) simulation suggested that the simulation systems reached equilibrium after 5 ns and that ACE and IAF can form complex in stabilization. Moreover, MD analysis revealed that the hydrogen bonds interactions between IAF and two key residues (His513 and Glu162) of ACE and the chelation between O3 atom of IAF and Zn^{2+} play more important roles in the stabilization for ACE–IAF complex, which might contribute significantly to the ACE inhibitory activity. Our study indicated that the novel and potential ACE inhibitory peptide IAF from pumpkin seed proteins can be considered as a promising candidate for controlling hypertension.

Keywords Pumpkin seed protein · Angiotensin-converting enzyme · ACE inhibitory peptide · In silico approach · Molecular dynamics simulation

Abbreviations

ACE	Angiotensin-converting enzyme
ADME	Absorption, distribution, metabolism, and elimination
FAPGG	N-[3-(2-furyl)acryloyl]-Phe-Gly-Gly
LINCS	Linear constraint solver
MD	Molecular dynamic
MOE	Molecular operating environment
PME	Particle mesh Ewald
RMSD	Root mean square deviation
RMSF	Root mean square fluctuation
*R*g	Radius of gyration
SASA	Solvent-accessible surface area

✉ Fuqiang Liang
fuqiangliang@nufe.edu.cn

[1] College of Food Science and Engineering, Nanjing University of Finance and Economics, Nanjing 210023, Jiangsu, China

Introduction

Pumpkin (*Cucurbita moschata*) seeds are one of the major oilseeds in the world, especially in China, which is one of the largest pumpkin producers. The primarily used of pumpkin seeds (almost 90%) is for edible oil extraction, producing a large quantity of by-products, which is pumpkin seed meal that contains 60–70% of protein [1]. The high protein content makes pumpkin seeds an attractive and promising source of plant proteins. However, as major components of by-products after oil extraction process, these pumpkin seed proteins are usually discarded or utilized as animal feeds.

In recent years, pumpkin seed proteins have attracted great attention not only due to its nutritional value but also its important role as a good source of bioactive peptides. Many studies have suggested that pumpkin seed protein hydrolysates exhibit various biological activities, such as antioxidant, antidiabetic, and hepatoprotective activity [2–5]. Moreover, a recent study demonstrated that the essential amino acids (EAA) composition of pumpkin seed proteins met the requirements that specified by FAO/WHO for pre-school children and adults [6]. Consequently, pumpkin seed proteins with desirable nutritionally

properties can be recognized as an innovative source of bioactive peptides.

The inhibition of ACE (EC 3.4.15.1) is an effective target for the control of hypertension, which is a serious public health problem worldwide. Food proteins-derived ACE inhibitory peptides, because of their easy absorption and importantly without undesirable adverse effects, thus could serve as an alternative of commercial antihypertensive drugs for the prevention of hypertension [7]. A previous study by Vaštag et al. reported that pumpkin seed proteins hydrolyzed by alcalase (EC 3.4.21.62) were found to show higher ACE inhibitory activity than by flavourzyme and the combined use of them [2]. As a commercially protease, alcalase has been extensively used in the production of ACE inhibitory peptides from diverse food proteins [8]. Hence, it can be hypothesized that alcalase is suitable for the generation of ACE inhibitory peptides from pumpkin seed proteins. 12S globulin and 2S albumin are two major fraction of pumpkin seed proteins [9]. However, the potential of pumpkin seed proteins hydrolyzed with alcalase to release bioactive peptides has not been studied systematically. Hence, efforts are needed to explore potent ACE inhibitory peptides from pumpkin seed proteins.

The traditional method to screen novel bioactive peptides contains a complex series of steps, which makes it time consuming and low efficiency [10]. Recently, in silico approach, as a result of the development of bioinformatic tools, such as BIOPEP-UWM database, SwissADME webtool, molecular docking and molecular dynamic simulation techniques, is emerging as a cost-effective, useful and valid tool [11, 12]. In silico approach has been widely used to predict and discover novel ACE inhibitory peptides released from various food proteins, such as rice bran protein [13], milk protein [14], and quinoa protein [15]. The aim of the present study was to predict and screen novel ACE inhibitory peptides from pumpkin seed proteins using the in silico approach and further to elucidate the underlying inhibition mechanism of ACE.

Materials and methods

Materials and reagents

ACE (A6778), N-[3-(2-furyl)acryloyl]-Phe-Gly-Gly (FAPGG, F7131) and 4-(2-hydroxyethyl)-1-piperazine ethanesulfonic acid (HEPES) were purchased from Sigma-Aldrich (St. Louis, MO, USA).

Evaluation of pumpkin seed proteins as precursors of bioactive peptides

Two sequences of pumpkin seed proteins, namely 11S globulin subunit beta (P13744) and 2S albumin (Q39649) (supplementary information (SI) Table S1), were retrieved from the UniProt Knowledgebase (http://www.uniprot.org/). Their potential to be the source of bioactive peptides were evaluated using the "Profiles of potential biological activity" of BIOPEP-UWM database (http://www.uwm.edu.pl/biochemia/index.php/pl/biopep). Then the occurrence frequency of peptide fragments with a given bioactivity in a protein sequence (A) is calculated based on the following equation:

$$A = a/N, \tag{1}$$

where a represents the number of fragments with a given bioactivity activity in a protein sequence, and N represents the number of amino acid resides in the protein.

In silico digestion of pumpkin seed proteins by alcalase

The "ENZYME(S) ACTION" tool in the BIOPEP-UWM database was used to hydrolyze the two pumpkin seed proteins by alcalase. The release frequency (A_E) of ACE inhibitory peptides and its relative release frequency (W) are calculated according to the following equations, respectively. Subsequently, di- and tripeptides without known ACE inhibitory activities were selected for the following study:

$$A_E = d/N, \tag{2}$$

$$W = A_E/A, \tag{3}$$

where d represents the number of peptide fragments with a given bioactivity activity released from the select protein sequence by alcalase, and N represents the number of amino acid resides in the protein.

Molecular docking

The structure of selected peptides was drawn by Molecular Operating Environment (MOE) software and their energies were minimized. The 3D structure of ACE in complex with lisinopril (PDB ID: 1O86, 2.00 Å) was download from the Protein Data Bank (https://www.rcsb.org). All water molecules in the crystal structure were removed and then subjected to structure preparation program of MOE. The redocking of lisinopril and the docking of peptides were performed with the followed parameters: Placement: Triangle matcher; rescoring 1: London dG; Refinement: Induced fit; and rescoring 2: GBVI/WSA dG.

The prediction of ADME properties and toxicity

The online tools SwissADME (http://www.swissadme.ch/) and ToxinPred (http://crdd.osdd.net/raghava//toxinpred/) were

used to predict the human gastrointestinal absorption (HIA) properties and the toxicity of these selected peptides.

Synthesis of peptide IAF

The peptide IAF (purity > 95%) was synthesized by Bankpeptide Biological Technology Co., Ltd. (Hefei, China) and was stored at − 20 °C until use.

Assay for ACE inhibitory activity

ACE inhibitory activity of IAF was determined according to the method described by Uraipong et al. [16] with modifications. Briefly, 10 µL of ACE solution (0.1 unit/mL in 80 mM HEPES) and 40 µL different concentrations of IAF were mixed in a 96-well microplate. The plate was incubated at 37 °C for 10 min and then 50 µL of 1.0 mM FAPGG was added into each well to start the reaction. The absorbance was monitored for 30 min at 340 nm. ACE inhibitory activity is calculated according to the following equation:

$$\mathrm{ACE}(\%) = \left[1 - \left(R/R_0\right)\right] \times 100, \quad (4)$$

where R and R_0 are the slopes of IAF and control, respectively.

MD simulations

MD simulations were performed using Amber99SB-ILDN force field of GROMACS software package version 2019.5 [17]. Each system (ACE–IAF complex and ACE protein) was solvated in SPC216 water in a dodecahedron box, with a minimum distance of 1.0 nm among the protein surfaces and the box edges. Na^+ ions were added to neutralize the system. The Particle Mesh Ewald (PME) method was used to evaluate the electrostatic interaction and the cutoff value for van der Waals interaction was set to 1.0 nm. Followed energy minimization using steepest descent method, 100 ps NVT and NPT equilibration were performed to reach the set temperature (300 K) and pressure (1 bar). 30 ns MD simulations of each system with a time step of 2 fs were performed.

Statistical analysis

Origin 8.0 and SPSS 13.0 were utilized for the data processing. Statistical significance was set at $P < 0.05$.

Results and discussions

Biological activity profiles of pumpkin seed proteins and ACE inhibitory peptides released after in silico proteolysis by alcalase

To evaluate the potential of pumpkin seed proteins as precursors of bioactive peptides, two predominant protein sequences including 11S globulin and 2S albumin were selected to determine the A values by BIOPEP-UWM database. As shown in SI table S2, fragments with 17 known bioactivity activities in total were found in pumpkin seed protein. The results were in agreement with some previous studies that have reported several biological activities of pumpkin seed protein hydrolysate, including antioxidant activity and ACE inhibitory activity [2, 18, 19]. Moreover, as shown in table S2, the frequency of ACE inhibitory peptides occurrence in 11S globulin ($A = 0.4662$) and 2S albumin ($A = 0.3616$) were higher than that of others except dipeptidyl peptidase IV inhibitory peptides. According to a previous study by Iwaniak et al. [20], the moderated A values in our study implied that pumpkin seed proteins could be considered as a source of various bioactive peptides, especially ACE inhibitors with a high potential. A_E is one important parameter that can be used to evaluate the release frequency of the bioactive fragments with a given bioactivity from a protein by selected enzymes. As shown in Table 1, the A_E value of 11S globulin was higher than that of 2S albumin, as a result of its high A value, suggesting that more ACE inhibitory peptides could be released by alcalase. According to the previous study [20], the A_E and W in the study suggested that alcalase might be suitable to release ACE inhibitory peptides from pumpkin seed proteins. The results is also in agreement with the experimental study by Vaštag et al. [2].

A total of 111 peptides (SI Fig. S1) in total can be released from the two protein sequences after in silico digestion with alcalase, and among which 16 peptides with known ACE inhibitory activities are listed in Table 1. ACE inhibitory peptide-derived food proteins have been extensively studied. To exert an inhibitory activity, it is necessary that peptides are absorbed, and reach the target tissue in an active form. Small molecular peptides, especially di-/tripeptides, were found to more likely to penetrate through intestinal membranes in their intact forms [21]. Thus, 47

Table 1 In silico proteolysis of pumpkin seed proteins by alcalase

Proteins	A_E	W	ACE-inhibitory peptides	Total number
11S globulin	0.0327	0.0743	RL (1), VF(3), MY(1), VW (2), PL (1), AF (1), GF (1), IF (1), KY (1), TE (1), EW (1), AGS (1)	15
2S albumin	0.0084	0.0244	VE (1)	1

peptides (shown in Table 2), including 20 tripeptides and 27 dipeptides, were selected for further screening study.

Virtual screening for novel ACE inhibitory peptides

To screen potential ACE inhibitory peptides, 47 peptides were docked to ACE using MOE software. First, the initial ligand, lisinopril, was extracted and re-docked into ACE to validate the accuracy of the docking algorithm. The root mean square deviation (RMSD) value between the re-docked ligand and the native ligand conformation was 0.83 Å (SI Fig. S2), which is less than 2 Å, indicating that the docking parameters to be used were reliable [22]. Table 2 shows the rank of *S* values of the 47 peptides. Peptides with lower docking score (S value) could be considered to be more potent ACE inhibitors. Results in Table 2 revealed that the docking scores of 15 peptides ($S < -11.5$), among the 47 selected peptides, were lower or comparable than the score of the origin inhibitor lisinopril (− 12.6746). Our results suggested that these peptides exhibited stronger binding affinity with ACE compared to the rest, hence, might be potential candidate for ACE inhibitors.

Many promising inhibitors fail to exhibit ACE inhibitory activities due to their unfavorable bioavailability characteristics [23]. Thus, the HIA properties of the top 15 scoring peptides were evaluated by SwissADME. According to the BOILED-Egg model (Fig. 1A), small molecules that presented in the white zone could passive absorption by the gastrointestinal tract with high likelihood, and that drawn by red circles cannot efflux by P-Glycoprotein (P-gp) [24]. Accordingly, only IAF (molecule 14 in Fig. 2A) was predicted to exhibit acceptable HIA properties, and to be not a PGP substrate (PGP-). Moreover, the bioavailability radar (Fig. 1B) shows that IAF has good physiochemical properties required for oral bioavailability [24]. Bioactive peptides with good bioavailability were presumed to exhibit high bioactivity [25]. Collectively, the above in silico results imply that IAF (structure shown in Fig. 1C) can be considered to be potential ACE inhibitors with good bioavailability. Therefore, the tripeptide IAF was selected for further study.

ACE inhibitory activity and mechanisms of IAF

Based on the above virtual screening results, IAF was chemically synthesized and its ACE inhibitory activity was evaluated by in vitro assay. According to the in vitro results (Fig. 2A), the IC_{50} value of IAF was 19.87 ± 0.50 μM. Obviously, the ACE inhibitory activity of IAF was higher than that of several previous identified, such as Ala-Phe (AF, IC_{50} = 165.3 μM) and Ile-Phe (IF, IC_{50} = 65.8 μM) from salt-free soy sauce [26], Val-Val-Leu-Tyr-Lys (VVLYK, IC_{50} = 533.9 μM) from oil palm kernel glutelin-2 [27], and Ala-Gly-Ser (AGS, IC_{50} = 527.9 μm) from cuttlefish (*Sepia officinalis*) muscle proteins [28]. Thus, the novel tripeptide IAF obtained in the study is one promising ACE inhibitor.

The active site of ACE consists of three major pockets: S1 (Ala354, Glu384 and Tyr523), S2′ (Gln281, Tyr520, Lys511, His513 and His353), and S1′ (Glu162) [29]. Further, molecular docking was conducted to investigate the binding mode between IAF and ACE. As shown in Fig. 2B, IAF formed hydrogen bonds with five key residues of ACE enzyme, including Tyr523, Glu384, Ala354 of S1, Glu162 of S1′ and His387. In addition, it can be seen that O2 and O3 atoms of IAF interacted with Zn ion (Zn^{2+}) at the active

Table 2 Docking scores and toxicity prediction of 47 peptides

No.	Peptide	*S* value	Toxicity	No.	Peptide	*S* value	Toxicity	No	.Peptide	*S* value	Toxicity
1	RKF	− 13.6466	Non-toxin	17	RD	− 11.3781	Non-toxin	33	IF	− 10.2626	Non-toxin
2	RRS	− 13.1023	Non-toxin	18	PGF	− 11.1364	Non-toxin	34	AGS	− 10.2134	Non-toxin
3	VRL	− 13.0397	Non-toxin	19	EW	− 11.1196	Non-toxin	35	VL	− 10.2131	Non-toxin
4	ERS	− 12.8224	Non-toxin	20	HW	− 11.0138	Non-toxin	36	QS	− 9.97613	Non-toxin
5	ENL	− 12.5210	Non-toxin	21	NAM	− 10.9469	Non-toxin	37	VQ	− 9.96635	Non-toxin
6	DGE	− 12.1990	Non-toxin	22	VNS	− 10.9192	Non-toxin	38	HS	− 9.96591	Non-toxin
7	NMY	− 12.1401	Non-toxin	23	GQS	− 10.8736	Non-toxin	39	VW	− 9.94495	Non-toxin
8	RIS	− 12.1316	Non-toxin	24	RQ	− 10.7969	Non-toxin	40	PL	− 9.90983	Non-toxin
9	IES	− 11.9947	Non-toxin	25	QGS	− 10.7671	Non-toxin	41	PW	− 9.90387	Non-toxin
10	TE	− 11.9941	Non-toxin	26	RS	− 10.6734	Non-toxin	42	ES	− 9.76137	Non-toxin
11	VE	− 11.9572	Non-toxin	27	DL	− 10.6487	Non-toxin	43	VF	− 9.67621	Non-toxin
12	EF	− 11.9271	Non-toxin	28	RL	− 10.6007	Non-toxin	44	PS	− 9.63882	Non-toxin
13	HTL	− 11.7874	Non-toxin	29	AGR	− 10.5928	Non-toxin	45	VS	− 9.20781	Non-toxin
14	IAF	− 11.7852	Non-toxin	30	KY	− 10.4939	Non-toxin	46	GF	− 9.19822	Non-toxin
15	VMY	− 11.7576	Non-toxin	31	MY	− 10.3978	Non-toxin	47	AF	− 8.99203	Non-toxin
16	PIL	− 11.4048	Non-toxin	32	KN	− 10.3914	Non-toxin	-	Lisinopril	− 12.6746	–

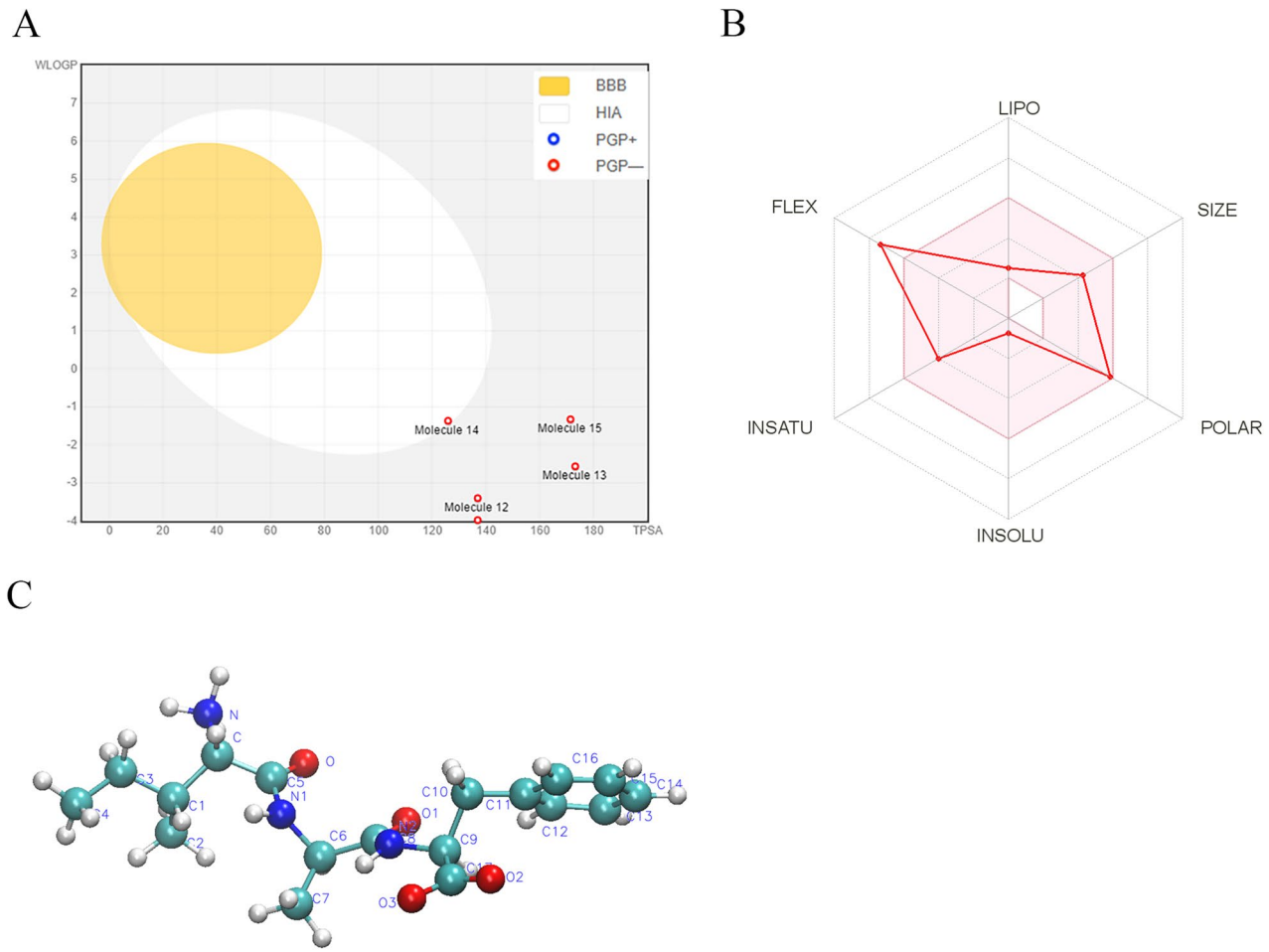

Fig. 1 ADME properties of 15 peptides. **A** The EGG-BOILED model for selected peptides. **B** The bioavailability radar of IAF. The pink area represents the most favorable area for six physicochemical properties including INSATU (unsaturation), INSOLU (insolubility), FLEX (rotatable bonds), LIPO (lipophilicity), SIZE (molecular weight) and POLAR (polar surface area). **C** Molecular structure of IAF

site (Fig. 2B, C). The distances between the oxygen atoms and Zn ion were 1.96 and 1.97 Å, respectively. This favors their interactions with Zn ion, which play significant roles in the inhibition of ACE enzyme [30]. This indicated that IAF can effectively interact with key residues at the active site of ACE.

Stability of ACE–IAF complex

To better understand the interaction molecular mechanisms between IAF and ACE, the 30 ns MD simulation of ACE–IAF complex was carried out using Gromacs software package. ACE–IAF complex with low binding energy was selected as starting structure to perform MD simulation. In addition, MD simulation of ACE without inhibitor IAF was also performed to compare with ACE–IAF complex. RMSD is a key parameter to reflect the stability of the simulation system, and its lower value indicates higher stability [31]. As shown in Fig. 3A, RMSD values of ACE and ACE–IAF complex tends to be stable after 5 ns, floating around 0.1785 and 0.1685 nm, respectively. Both of them were less than 0.2 nm reveal that the two simulation systems achieved equilibrium [17]. It can be observed that RMSD value of ACE without IAF was higher than that of ACE–IAF complex, suggesting that ACE combined with the inhibitor was more stable than that without. Moreover, the motion trajectory of IAF was analyzed and the results is presented in Fig. 3B. Together with the RMSD value of IAF shown in Fig. 3A, the results suggested that IAF did not escape from the docking cavity of ACE during the 30 ns simulation. In addition, the radius of gyration (*R*g) values, as an indicator for structural change in a protein, was calculated to evaluate structural changes of ACE. The average *R*g values after 5 ns simulation are 2.3990 nm for ACE and 2.3944 nm for ACE–IAF complex, respectively (Fig. 3C). Similarly, as shown in Fig. 3D, the binding of IAF to ACE does not induce a remark change

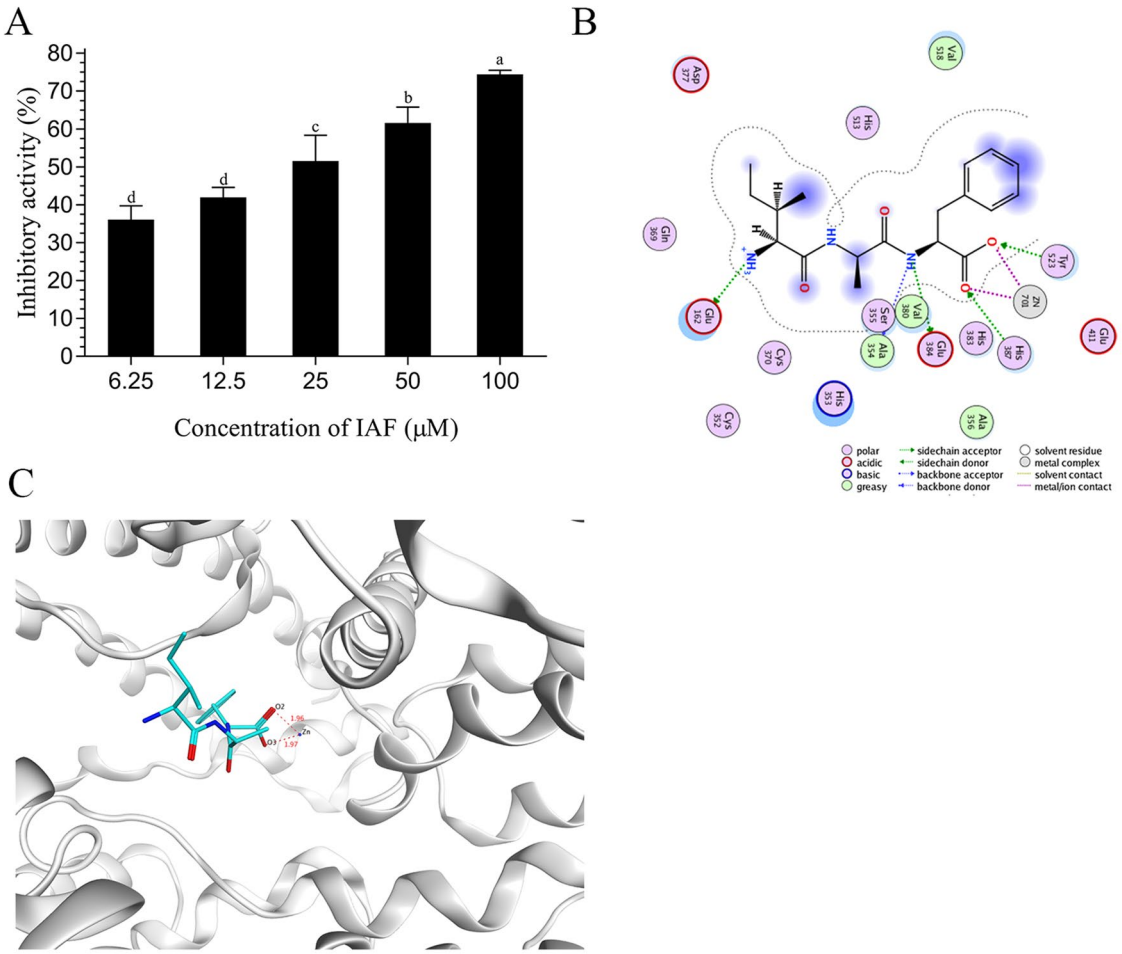

Fig. 2 Inhibitory activity and interaction mechanism of IAF. **A** In vitro inhibitory activity of ACE by IAF. **B** 2D interactions of IAF with the residues in the active site of ACE. **C** Interactions between IAF and Zn^{2+} in the active site of ACE

in the solvent-accessible surface area (SASA) of ACE. As depicted, the change of *R*g and SASA is less than 0.2%, indicating that the overall structure of ACE remained stable during simulation.

The root mean square fluctuation (RMSF) is an important indicator of the average fluctuations of every amino acid residue [17]. Thus, RMSF was further calculate to investigate the freedom of motion for per residue of ACE protein. Figure 3E, F displays the RMSF values of the two systems during the 30 ns simulation and the location of flexible resides (His153-Gly156, Phe293-Asp300 and Ser435-Gly438) on ACE protein. As expected, these residues belonging to loops mostly fluctuated during two simulations on the surface of ACE. The amino acid residues at the active site of ACE did not exhibit a high RMSF value. Taken together, the above results indicate that the overall conformation of ACE protein was stable over the simulation time when the peptide IAF is bound, and therefore, ACE–IAF was able to form stable conformation at the active site of ACE.

Interactions of IAF with ACE

It is well known that the non-covalent interactions between ACE and its inhibitory peptides were essential factors contributed to the inhibition of ACE. The last frame of MD was used to analysis the non-covalent interactions between IAF and ACE. As shown in Fig. 4A, B, IAF formed four hydrogen bonds with residues Ala354, Arg522, Glu162 and His513 after 30 ns simulation, which is different form the molecular docking results. It was reported that a hydrogen bond is considered to be stable when its occupancy rate is higher than 50% [32]. Therefore, the hydrogen bond occupancy of IAF and ACE were calculated to evaluate the strength and stability of hydrogen bonds. As summarized in Table 3, three hydrogen bonds were found to be remain stable during the simulation for their occupancy were higher than 50%. In consistently, it can be seen that ACE–IAF complex were mainly stabilized by 3 ~ 5 hydrogen bonding after 5 ns simulation (Fig. 4C), indicating that continuous

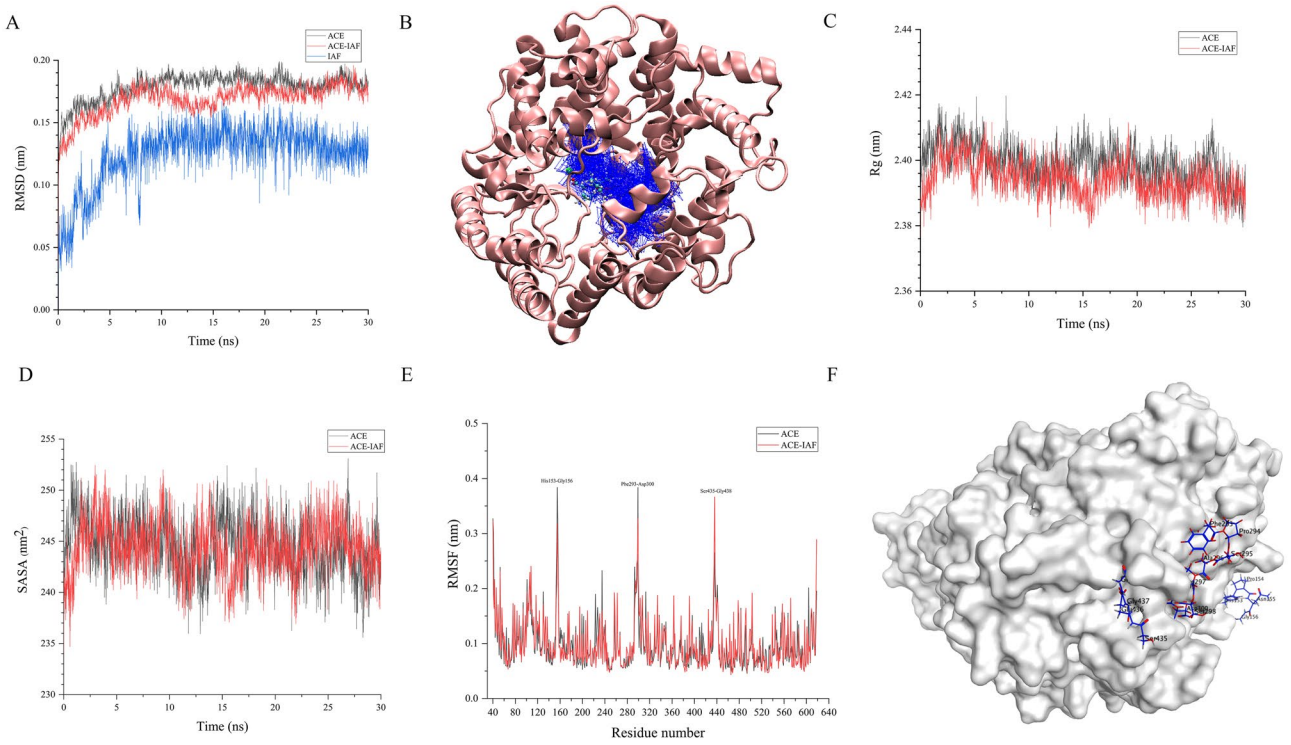

Fig. 3 Stability of ACE–IAF complex. The RMSD (**A**), Rg (**C**), SASA (**D**), and RMSF (**E**) values of ACE and IAF (blue line in **A**) during the 30 ns MD simulation. **F** Molecular surface of ACE in simulation. The last frame was used to calculate. **B** The motion trajectory of IAF (line in blue) in the binding cavity over the 30 ns MD simulation

hydrogen bonds formed between ACE and IAF. Based on Fig. 4D, it can be implied that the interactions between IAF and His513 and Glu162 play more important roles among the three hydrogen bonds listed in Table 3 for their distances are more stable during the simulation. Meanwhile, IAF can formed hydrophobic interactions with His353, Ser355, Val518, Pro519, Tyr523, His383, Val380, Glu384, Glu411 and Gln369 (Fig. 4B). Many of these interacted amino acids has been demonstrated to be key residues in ACE active site which interact with ACE inhibitor lisinopril such as His383, Glu411, Tyr523 and Glu384 [33]. These results indicate that IAF can effectively interact with ACE at the active site through hydrogen bonds and hydrophobic interactions, which can partly explain the ACE inhibitory activity of IAF.

Interactions of IAF with Zn^{2+} in ACE

An increasing number of studies have confirmed that the interactions between ACE inhibitors and Zn^{2+} exhibits significant influence on the inhibition of ACE [17, 34]. The interaction between Zn^{2+} in ACE and IAF is shown in Fig. 5A. As shown, the Zn^{2+} is surrounded by three residues, namely Glu411, Glu384 of ACE and Phe of IAF. The crucial roles of Glu411 and Glu384 for the inhibition of ACE has been reported in previous studies [35, 36]. Different with the molecular docking (Fig. 2B, C), the metal carboxylic coordination bond between O2 atom of IAF was found to be broken after 30 ns simulation. It is known that a shorter distance or closer proximity is essential for forming ligand–Zn^{2+} interaction [34]. Thus, the distance between the oxygen atoms, including O2 and O3 of IAF, OE1 and OE2 of Glu411, and OE2 of Glu384 and Zn^{2+}, were further calculate. As shown in Fig. 5B–D, the average mean values of distance between four oxygen atoms and Zn^{2+} after 5 ns simulation were 0.3284, 0.1776, 0.1879, 0.1837 and 0.1843 nm, respectively. Except the distance between O2 atom of IAF and Zn^{2+}, three of them were less than 0.214 nm which is the sum of radius of oxygen atom (0.14 nm) and Zn^{2+} (0.074 nm). Therefore, in consistent with Fig. 5A, the Zn^{2+} and carboxyl groups are capable of forming four metal carboxylic coordination bonds, which play important roles for the stability of ACE–IAF complex [30]. According to a previous report by Natesh et al. [37], the formation of metal carbonyl bond between Zn^{2+} and enalapril, a commercial antihypertensive drug, brings about the observed ACE inhibiting behavior. Moreover, it is difficult to break the chelation interactions because of the higher energy than other interaction forces [30]. Our results show that the average distance value between Zn^{2+} and O3 atom of

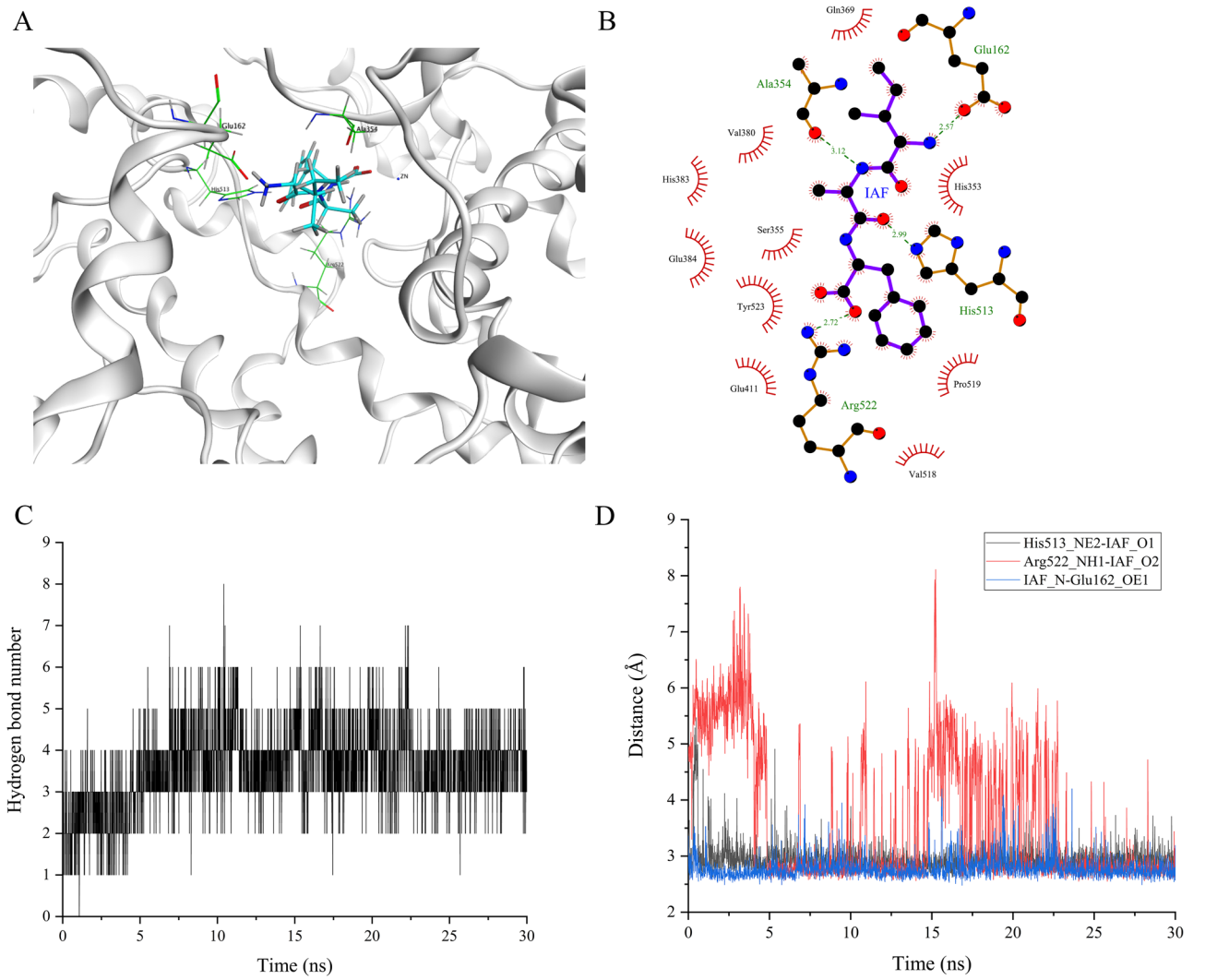

Fig. 4 Interactions of IAF with ACE. **A** Orientation of IAF at the active site of ACE. **B** Hydrogen bonding interactions between IAF and ACE resides obtained from the last frame of simulation. **C** Hydrogen bond numbers in ACE–IAF simulation system. **D** Distances between atoms of IAF and key residues of ACE

Table 3 List of hydrogen bonds observed between the IAF with ACE during the simulation

Hydrogen bond donor	Hydrogen bond acceptor	Occupancy (%)
HIS513-Side-NE2	lig620-Side-O1	67.11
ARG522-Side-NH1	lig620-Side-O2	63.43
lig620-Main-N	GLU162-Side-OE1	61.71

IAF favors the formation of chelation interaction during the 30 ns simulation. Consequently, we can infer that its chelation with Zn^{2+} in the active site plays an important role in the ACE inhibition by IAF.

Conclusions

The novel ACE inhibitory peptide IAF was successfully identified from pumpkin seed proteins in this study. IAF exhibited potent in vitro ACE inhibitory ability with an IC50 of 19.87 ± 0.50 μM. MD simulations suggest that ACE–IAF complex reached stable after 5 ns and the structure of ACE protein remain stable when the inhibitor IAF is bounded. Hydrogen bond interactions between IAF and key residues (His513 and Glu162) of ACE including, in particular, the formation of metal carboxylic coordination bond between O3 atom of IAF and Zn^{2+} were considered to play critical roles in the stabilization of ACE–IAF complex, which may be partly explain the considerable inhibition of ACE by IAF. Further studies including ex vivo and in vivo experiments would be necessary to investigate

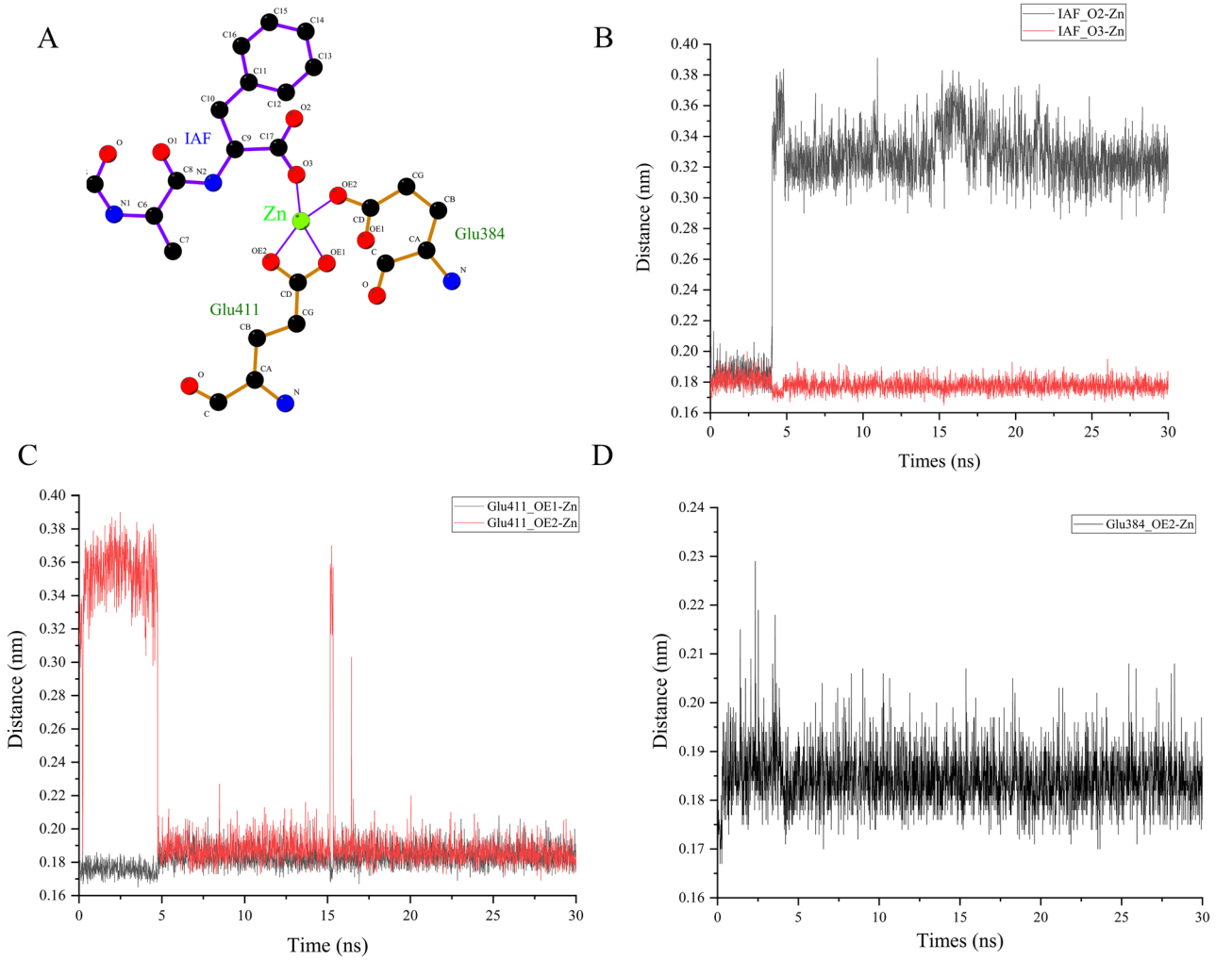

Fig. 5 The intermolecular interaction mechanisms between IAF and ACE. **A** Binding mode between Zn^{2+} and IAF and ACE resides (Glu384 and Glu411). **B** The distance between Zn^{2+} and O3 of IAF with time dependence. **C** The distance between Zn^{2+} and OE1 and OE2 of Glu411 with time dependence. **D** The distance between Zn^{2+} and OE2 of Glu384 with time dependence

the efficacy of IAF for controlling blood pressure and hypertension.

Supplementary Information The online version contains supplementary material available at https://doi.org/10.1007/s00217-021-03783-1.

Funding This work was supported by [National Natural Science Foundation of China] (Grant number 32001702).

Declarations

Conflict of interest The authors have no relevant financial or non-financial interests to disclose.

Compliance with ethics requirements This study does not contain any studies with human participants or animals performed by any of the authors.

References

1. Venuste M, Zhang X, Shoemaker CF et al (2013) Influence of enzymatic hydrolysis and enzyme type on the nutritional and antioxidant properties of pumpkin meal hydrolysates. Food Funct 4:811–820. https://doi.org/10.1039/c3fo30347k
2. Vaštag Ž, Popović L, Popović S et al (2011) Production of enzymatic hydrolysates with antioxidant and angiotensin-I converting

enzyme inhibitory activity from pumpkin oil cake protein isolate. Food Chem 124:1316–1321. https://doi.org/10.1016/j.foodchem.2010.07.062
3. Xia HC, Li F, Li Z, Zhang ZC (2003) Purification and characterization of Moschatin, a novel type I ribosome-inactivating protein from the mature seeds of pumpkin (*Cucurbita moschata*), and preparation of its immunotoxin against human melanoma cells. Cell Res 13:369–374. https://doi.org/10.1038/sj.cr.7290182
4. Caili F, Huan S, Quanhong L (2006) A review on pharmacological activities and utilization technologies of pumpkin. Plant Foods Hum Nutr 61:73–80. https://doi.org/10.1007/s11130-006-0016-6
5. Ozuna C, León-Galván MF (2017) Cucurbitaceae seed protein hydrolysates as a potential source of bioactive peptides with functional properties. Biomed Res Int 2017:2121878. https://doi.org/10.1155/2017/2121878
6. Vinayashree S, Vasu P (2021) Biochemical, nutritional and functional properties of protein isolate and fractions from pumpkin (*Cucurbita moschata* var Kashi Harit) seeds. Food Chem 340:128177. https://doi.org/10.1016/j.foodchem.2020.128177
7. Miralles B, Amigo L, Recio I (2018) Critical review and perspectives on food-derived antihypertensive peptides. J Agric Food Chem 66:9384–9390. https://doi.org/10.1021/acs.jafc.8b02603
8. Tacias-Pascacio VG, Morellon-Sterling R, Siar EH et al (2020) Use of alcalase in the production of bioactive peptides: a review. Int J Biol Macromol 165:2143–2196. https://doi.org/10.1016/j.ijbiomac.2020.10.060
9. Bučko S, Katona J, Popović L et al (2016) Influence of enzymatic hydrolysis on solubility, interfacial and emulsifying properties of pumpkin (*Cucurbita pepo*) seed protein isolate. Food Hydrocoll 60:271–278. https://doi.org/10.1016/j.foodhyd.2016.04.005
10. Han R, Maycock J, Murray BS, Boesch C (2019) Identification of angiotensin converting enzyme and dipeptidyl peptidase-IV inhibitory peptides derived from oilseed proteins using two integrated bioinformatic approaches. Food Res Int 115:283–291. https://doi.org/10.1016/j.foodres.2018.12.015
11. Iwaniak A, Darewicz M, Mogut D, Minkiewicz P (2019) Elucidation of the role of in silico methodologies in approaches to studying bioactive peptides derived from foods. J Funct Foods 61:103486. https://doi.org/10.1016/j.jff.2019.103486
12. Minkiewicz P, Iwaniak A, Darewicz M (2019) BIOPEP-UWM database of bioactive peptides: current opportunities. Int J Mol Sci 20:5978. https://doi.org/10.3390/ijms20235978
13. Pooja K, Rani S, Prakash B (2017) In silico approaches towards the exploration of rice bran proteins-derived angiotensin-I-converting enzyme inhibitory peptides. Int J Food Prop 20:2178–2191. https://doi.org/10.1080/10942912.2017.1368552
14. Fitzgerald RJ, Cermeño M, Khalesi M et al (2020) Application of in silico approaches for the generation of milk protein-derived bioactive peptides. J Funct Foods 64:103636. https://doi.org/10.1016/j.jff.2019.103636
15. Guo H, Richel A, Hao Y et al (2020) Novel dipeptidyl peptidase-IV and angiotensin-I-converting enzyme inhibitory peptides released from quinoa protein by in silico proteolysis. Food Sci Nutr 8:1415–1422. https://doi.org/10.1002/fsn3.1423
16. Uraipong C, Zhao J (2016) Rice bran protein hydrolysates exhibit strong in vitro α-amylase, β-glucosidase and ACE-inhibition activities. J Sci Food Agric 96:1101–1110. https://doi.org/10.1002/jsfa.7182
17. Jiang Z, Zhang H, Bian X et al (2019) Insight into the binding of ACE-inhibitory peptides to angiotensin-converting enzyme: a molecular simulation. Mol Simul 45:215–222. https://doi.org/10.1080/08927022.2018.1557327
18. Mazloomi SN, Sadeghi-Mahoonak A, Ranjbar-Nedamani E, Nourmohammadi E (2019) Production of antioxidant peptides through hydrolysis of paper skin pumpkin seed protein using pepsin enzyme and the evaluation of their functional and nutritional properties. ARYA Atheroscler 15:218–227. https://doi.org/10.22122/arya.v15i5.1755
19. Vaštag Ž, Popović L, Popović S et al (2013) In vitro study on digestion of pumpkin oil cake protein hydrolysate: evaluation of impact on bioactive properties. Int J Food Sci Nutr 64:452–460. https://doi.org/10.3109/09637486.2012.749837
20. Iwaniak A, Minkiewicz P, Pliszka M et al (2020) Characteristics of biopeptides released in silico from collagens using quantitative parameters. Foods 9:1–29. https://doi.org/10.3390/foods9070965
21. Shen W, Matsui T (2017) Current knowledge of intestinal absorption of bioactive peptides. Food Funct 8:4306–4314. https://doi.org/10.1039/C7FO01185G
22. Meng L, Feng K, Ren Y (2018) Molecular modelling studies of tricyclic triazinone analogues as potential PKC-θ inhibitors through combined QSAR, molecular docking and molecular dynamics simulations techniques. J Taiwan Inst Chem Eng 91:155–175. https://doi.org/10.1016/j.jtice.2018.06.017
23. Abdelhedi O, Nasri M (2019) Basic and recent advances in marine antihypertensive peptides: production, structure-activity relationship and bioavailability. Trends Food Sci Technol 88:543–557. https://doi.org/10.1016/j.tifs.2019.04.002
24. Daina A, Zoete V (2016) A boiled-egg to predict gastrointestinal absorption and brain penetration of small molecules. ChemMedChem 11:1117
25. Gianfranceschi GL, Gianfranceschi G, Quassinti L, Bramucci M (2018) Biochemical requirements of bioactive peptides for nutraceutical efficacy. J Funct Foods 47:252–263. https://doi.org/10.1016/j.jff.2018.05.034
26. Zhu X-L, Watanabe K, Shiraishi K et al (2008) Identification of ACE-inhibitory peptides in salt-free soy sauce that are transportable across caco-2 cell monolayers. Peptides 29:338–344. https://doi.org/10.1016/j.peptides.2007.11.006
27. Zheng Y, Li Y, Zhang Y et al (2017) Purification, characterization, synthesis, in vitro ACE inhibition and in vivo antihypertensive activity of bioactive peptides derived from oil palm kernel glutelin-2 hydrolysates. J Funct Foods 28:48–58. https://doi.org/10.1016/j.jff.2016.11.021
28. Balti R, Nedjar-Arroume N, Adjé EY et al (2010) Analysis of novel angiotensin I-converting enzyme inhibitory peptides from enzymatic hydrolysates of cuttlefish (*Sepia officinalis*) muscle proteins. J Agric Food Chem 58:3840–3846. https://doi.org/10.1021/jf904300q
29. Yu Z, Wang L, Wu S et al (2021) In vivo anti-hypertensive effect of peptides from egg white and its molecular mechanism with ACE. Int J Food Sci Technol 56:1030–1039. https://doi.org/10.1111/ijfs.14756
30. Qi C, Zhang R, Liu F et al (2017) Molecular mechanism of interactions between inhibitory tripeptide GEF and angiotensin-converting enzyme in aqueous solutions by molecular dynamic simulations. J Mol Liq 249:389–396
31. Nawaz KAA, David SM, Murugesh E et al (2017) Identification and in silico characterization of a novel peptide inhibitor of angiotensin converting enzyme from pigeon pea (*Cajanus cajan*). Phytomedicine 36:1–7. https://doi.org/10.1016/j.phymed.2017.09.013
32. Desheng L, Jian G, Yuanhua C et al (2011) Molecular dynamics simulations and MM/GBSA methods to investigate binding mechanisms of aminomethylpyrimidine inhibitors with DPP-IV. Bioorg Med Chem Lett 21:6630–6635
33. Aiemratchanee P, Panyawechamontri K, Phaophu P et al (2020) In vitro antihypertensive activity of bioactive peptides derived from porcine blood corpuscle and plasma proteins. Int J Food Sci Technol. https://doi.org/10.1111/ijfs.14853
34. Shi A, Liu H, Liu L et al (2014) Isolation, purification and molecular mechanism of a peanut protein-derived ACE-inhibitory

peptide. PLoS ONE 9:23–25. https://doi.org/10.1371/journal.pone.0111188
35. Wang X, Wu S, Xu D et al (2011) Inhibitor and substrate binding by angiotensin-converting enzyme: quantum mechanical/molecular mechanical molecular dynamics studies. J Chem Inf Model 51:1074–1082
36. Jalkute CB, Barage SH, Dhanavade MJ, Sonawane KD (2013) Molecular dynamics simulation and molecular docking studies of angiotensin converting enzyme with inhibitor lisinopril and amyloid beta peptide. Protein J 32:356–364. https://doi.org/10.1007/s10930-013-9492-3
37. Natesh R, Schwager SLU, Evans HR et al (2004) Structural details on the binding of antihypertensive drugs captopril and enalaprilat to human testicular angiotensin I-converting enzyme. Biochemistry 43:8718